Magnetic order and superconductivity in $YBa_2Cu_{3-y}M_yO_z$ (M = Fe,Co)

D. Hechel, I. Nowik, E. R. Bauminger, and I. Felner
Racah Institute of Physics, The Hebrew University, Jerusalem 91904, Israel
(Received 20 March 1990)

Mössbauer studies, magnetic susceptibility, and powder x-ray diffraction were used to study the magnetic properties and superconductivity of $YBa_2Cu_{3-y}M_yO_z$ (M = Fe, Co) in both oxygen-rich and oxygen-deficient samples. T_c is reduced by increasing the dopant concentration and the analysis of Mössbauer spectra at different temperatures shows that antiferromagnetism in the Cu(2) site is found at concentrations where superconductivity disappears. It means that the materials exhibit either superconductivity or antiferromagnetic order in the Cu(2) site, depending on composition. The phase diagrams obtained are very similar to the well-known oxygen content phase diagram. For $z=6$ and $y \geq 0.5$, and for M = Co also with $z=7$, two independent magnetic transition temperatures have been observed. Both $T_{N1} \sim 400$ K and $T_{N2} \sim 220$ K, which correspond to the Cu(2) and Cu(1) sites, respectively, change very little with y.

I. INTRODUCTION

A central issue regarding high-T_c superconductivity is whether or not magnetic interactions are important in stabilizing the superconducting electronic ground state as suggested in many proposed theories.[1] Experimentally it is found that long-range antiferromagnetic (AFM) order of the Cu(2) planes exists in the nonsuperconducting $YBa_2Cu_3O_6$,[2] which leaves open the possibility that AFM correlations may persist into the superconducting (SC) phase. The SC-AFM phase diagram of $YBa_2Cu_3O_z$ with oxygen content (z) is now well established. This phase diagram shows[3] that for $6.4 < z < 7.0$ the system is orthorhombic, metallic, and superconducting with T_c being depressed as z decreases. For $z < 6.4$ the system is tetragonal, semiconducting, and AFM with $T_N \sim 410$ K for $z=6$ and decreasing as z increases. Using the Mössbauer technique on iron-doped samples, we have shown[4] that T_N is not affected by the presence of Fe and that Fe is thus a reliable probe of the magnetic behavior of the Cu(2) sites. In a recent paper we have shown that this phase diagram is not unique and substitution of Y by Pr leads in the $Y_{1-x}Pr_xBa_2Cu_3O_7$ system to a SC-AFM phase diagram as a function of x — very similar to that mentioned above— even though the materials are oxygen rich.[5] Measurements in the oxygen-deficient samples of the $Y_{1-x}Pr_xBa_2Cu_3O_6$ system show[5] that the Cu(2) site is AFM for all x values, and T_N varies little with x; $T_N(x=0)=415$ K and $T_N(x=1)=350$ K.

The phase diagram of $(La,M)_2CuO_4$ which resembles that of $YBa_2Cu_3O_7$, exhibits also dramatic behavior such as structural change, 3D antiferromagnetism, disordered magnetism, and superconductivity as a function of hole doping.[6] Also, in the third class of high-T_c superconductors, Bi-Sr-Cu-Ca-O, substitution of Y for Ca changes the electronic and magnetic properties and a quite similar phase diagram involving superconductivity and magnetism is obtained.[7] All these examples indicate that antiferromagnetism is commonly found in all these oxides in a series of compositions which exhibit super-conductivity for another series of composition. There is no conclusive evidence for coexistence of both phenomena at the same composition.[8] From an experimental viewpoint, a complete understanding of the high T_c superconductivity must include more information on the magnetic properties of the Cu-oxide base layer.

It has been reported by several groups that partial substitution of Cu in $YBa_2Cu_3O_7$ by Fe and Co progressively decreases T_c of the system; for iron or cobalt concentration exceeding 13 at. % the materials are not superconducting[9] even in the oxygen-rich compounds. The Fe and Co atoms were found to occupy predominantly the Cu(1) site with an increasing fraction occupying the Cu(2) sites as the total amount of dopant increased.[10] The main goal of the present paper is to show that in the oxygen-rich system $YBa_2Cu_{3-7}M_yO_7$ with M = Fe and Co and the value of y being close to the value of the disappearance of SC, a static magnetic ordering of the Cu(2) sites is induced. This system behaves in a way which is similar to the appearance of AFM order by removal of oxygen or substitution of Pr for Y.

In the oxygen-deficient $YBa_2Cu_{3-y}M_yO_z$ (M = Fe, Co) samples a second long-range AFM order develops on the Cu(1) chain sites. For $y \geq 0.5$ the high concentration of magnetic Fe ions which preferentially occupy the Cu(1) site induces magnetic order in this site with $T_N \sim 220$ K. The magnetic order with $T_N = 420$ K corresponds to the Cu(2) site. The two magnetic sublattices are practically decoupled.

II. EXPERIMENTAL DETAILS

The ceramic systems, $YBa_2Cu_{3-y}Co_yO_z$ doped with 1% of ^{57}Fe and $YBa_2Cu_{3-y}Fe_yO_z$ were prepared by conventional methods.[11] The oxygen-deficient samples were obtained by quenching the samples from 900 °C to liquid

nitrogen. X-ray diffraction studies were performed to determine the crystallographic structure and to insure the purity of the compounds. The Mössbauer spectroscopy studies were performed using a conventional constant-acceleration spectrometer and a 100 mCi ^{57}Co:Rh source. The spectra at various temperatures were least-square fitted with several subspectra corresponding to the various inequivalent iron sites. dc susceptibility measurements in low fields as a function of temperature were carried out in a PAR vibrating sample magnetometer to determine T_c of the samples. The magnetization measurements at 1 kOe were measured by a commercial SHE superconducting quantum interference device magnometer.

III. EXPERIMENTAL RESULTS AND DISCUSSION

A. Crystal structure measurement

X-ray powder-diffraction measurements on $YBa_2Cu_{3-y}M_yO_z$ samples indicate that all the samples are single phases and have the same tetragonal structure with a $P4/mmm$ space group (Table I). The $YBa_2Cu_{2.25}Fe_{0.75}O_6$ sample contains approximately 4% extra lines. For the full oxygenated samples, the a lattice parameters increase and the c lattice parameter decreases slightly with y. Remarkably, the cell volume increases as oxygen is removed. The total increase is about 1% and is mainly because of the expansion of the unit cell along the c direction. Since Fe and Co have a larger valence than Cu, they attract oxygen to maintain charge neutrality. Therefore we assign $z=7+\delta$ for the oxygen rich samples and $z=6+\delta$ for the quenched samples. The values of δ are proportional to y, and are not necessarily the same for $z=7$ and $z=6$ systems.

B. Superconductivity and antiferromagnetism in $YBa_2Cu_{3-y}Co_yO_{z+\delta}$ with $z=7$ and 6

The substitution of Cu by Co in the oxygen-rich $YBa_2Cu_3O_7$ produces drastic changes in T_c. It is well established that T_c decreases continuously to less than 4.2 K for $y=0.4$. With $y>0.4$ the compounds are not superconducting any more. T_c obtained for $YBa_2Cu_{2.8}Co_{0.2}O_{7+\delta}$ was 60 K in perfect agreement with published data.[12] On the other hand, $YBa_2Cu_{2.2}Co_{0.8}O_{7+\delta}$ was found not to be superconducting. Figure 1 displays the Mössbauer spectra of the two oxygen-rich samples at 90 K. The sextet in the sample with $y=0.8$ is due to Fe in the Cu(2) sites. This amounts to 27% of the overall iron. As the temperature is raised the magnetic splitting decreases until $T_N=380$ K, where the sextet disappears. Mössbauer studies[4] indicate that T_N of the Cu(2) sites is not affected by the presence of iron impurities. Therefore, this is another example of the competition between superconductivity and AFM where at levels of concentration where the superconductivity disappears the Cu moments order AFM in the CuO_2 planes. The details of the magnetic order of this compound will be discussed later.

No magnetic splitting is observed in the superconducting $YBa_2Cu_{2.8}Co_{0.2}O_{7+\delta}$ sample at 90 K (Fig. 1). The spectrum obtained is composed of four quadrupole doublets corresponding to four inequivalent iron (cobalt) sites due to different oxygen-neighbor configurations in the Cu(1) site.[13] Two doublets (each of about 30% of the area) with isomer shifts $S_{IS}=0.121(1)$ and 0.043 mm/s relative to Fe metal show quadrupole splitting of $\frac{1}{2}eqQ=2.05(2)$ and 0.98(2) mm/s. They are attributed to square planar coordinated Fe [Fig. 2(a)] which is the most populated oxygen configuration at the Cu(1) site in the $YBa_2Cu_3O_7$ phase,[13-14] and to the pyramidal configuration [Fig. 2(b)] in which three oxygens are in the plane (see also Fig. 9). The third doublet (about 15% of the area) with $\frac{1}{2}eqQ=1.51(2)$ and $S_{IS}=0.028(1)$ mm/s is associated with the tetrahedral configurations [Fig. 2(c)]. Finally a doublet with $\frac{1}{2}eqQ=0.62(2)$ mm/s and $S_{IS}=0.345$ mm/s corresponds to the octahedral configuration [Fig. 2(d)] and to Fe in the Cu(2) sites. Note that the quadrupole splittings obtained here are quite similar to those observed in iron-doped samples,[13-14] but the isomer shifts are different due to different electron densities at the Fe nuclei in the Cu(1) site.

In the quenched sample, which is not superconducting, we observe a well-defined magnetic sextet which accounts for about 17% of the spectral area (Fig. 3). We attribute this sextet to iron which replaces copper in the Cu(2) site and orders antiferromagnetically.[4] All iron atoms in the Cu(2) site are equivalent in terms of oxygen environment and yield a well-defined magnetic spectrum. At 90 K the magnetic hyperfine field is 460(5) kOe and the quadrupole interaction is $\frac{1}{2}eqQ=-0.35$ mm/s. As the temperature is raised, the magnetic splitting decreases and above $T_N=395$ K (Table I) the sextet disappears. The hyperfine

TABLE I. Lattice and magnetic hyperfine parameters for $YBa_2Cu_{3-y}M_yO_z$. All the H_{eff} values obtained at 90 K.

Compound	Lattice parameters a (Å)	c (Å)	V (Å^3)	Magnetic hyperfine parameter T_{N1} (K)	H_{eff} (kOe)	T_{N2} (K)	H_{eff} (kOe)
$YBa_2Cu_{2.8}Co_{0.2}O_{7+\delta}$	3.879(2)	11.70(1)	176.11	$T_c=60$ K			
$YBa_2Cu_{2.8}Co_{0.2}O_{6+\delta}$	3.873	11.77	176.51	395(5)	460(5)		
$YBa_2Cu_{2.2}Co_{0.8}O_{7+\delta}$	3.882	11.69	176.12	380(10)	500(5)	200(20)	152(5)
$YBa_2Cu_{2.2}Co_{0.8}O_{6+\delta}$	3.887	11.71	176.94	435(5)	493(5)	300(20)	265(5)
$YBa_2Cu_{2.5}Fe_{0.5}O_{7+\delta}$	3.875	11.66	175.11	330(10)	490(5)		
$YBa_2Cu_{2.5}Fe_{0.5}O_{6+\delta}$	3.880	11.76	177.10	420(10)	494(5)	220(20)	229(5)
$YBa_2Cu_{2.25}Fe_{0.75}O_{7+\delta}$	3.881	11.63	175.12	390(10)	496(5)		
$YBa_2Cu_{2.25}Fe_{0.75}O_{6+\delta}$	3.879	11.74	176.73	430(15)	495(5)	210(20)	296(5)

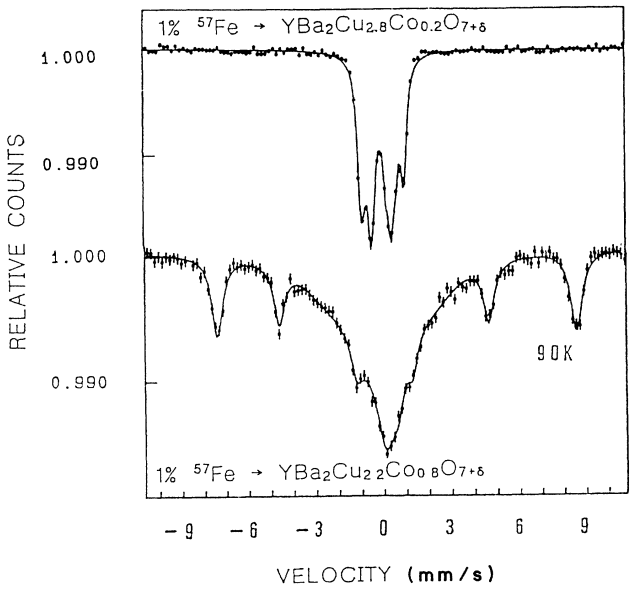

FIG. 1. Mössbauer spectra of oxygen-rich $YBa_2Cu_{3-y}Co_yO_{7+\delta}$ at 90 K.

fields as a function of temperature are shown in Fig. 4 (dashed line). The electric-field gradient at the Cu(2) site according to point-charge-model calculations, should be positive and point along the c axis. The measured negative-effective-quadrupole interaction indicates that the magnetic moments of the Cu(2) site lie in the basal plane.[2,4]

The central part of the spectra of Fig. 3 is fitted by three pairs of symmetric doublets with approximately the same parameters as in the oxygen-rich superconducting sample. It is noticeable that as the sample becomes oxygen deficient, the intensity of the planar configuration [Fig. 2(a)] is increased from 30% to 52% and that of the tetrahedral configuration [Fig. 2(c)] is increased from 15% to 20%. Note the additional doublet observed at

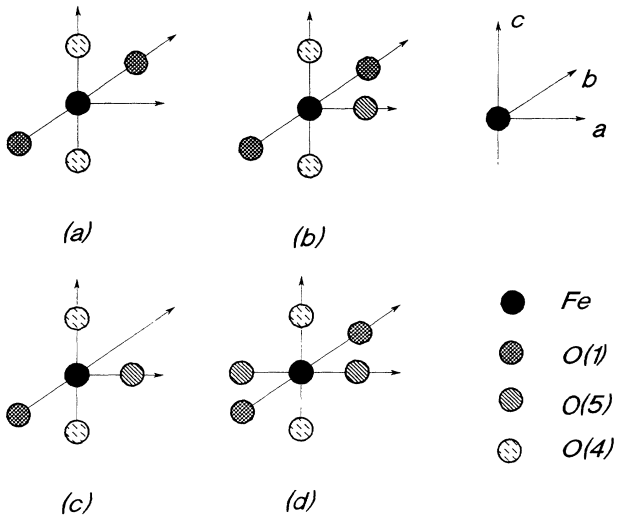

FIG. 2. Possible local environment of Fe at the Cu(1) site.

400 K (Fig. 4) above T_N with an intensity of about 20% and an $S_{IS}=0.25(1)$ mm/s and $\frac{1}{2}eqQ=0.67(1)$ mm/s. This doublet corresponds to iron in the Cu(2) sites and is obtained after the magnetic sextet has collapsed.

A different magnetic structure for $YBa_2Cu_{2.8}Co_{0.2}O_{6+\delta}$ was proposed[15] from neutron-scattering experiments. Two magnetic transitions were found: one at $T_{N1}=211$ K corresponding to the Cu(1) site and the other at $T_{N2}=415$ K corresponding to the Cu(2) site. Our results (Fig. 3) show clearly the existence of only one magnetic transition at about 400 K which is related to the Cu(2) site.

C. Two magnetic sublattices in $YBa_2Cu_{2.2}Co_{0.8}O_{z+\delta}$ with $z=7$ and 6

It is assumed that more than 80% of Co ions enter the Cu(1) chain at site.[10] This means that for $y=0.8$ about $\frac{2}{3}$ of the Cu(1) site is occupied by the magnetic Co ions which should encourage magnetic ordering on the chain

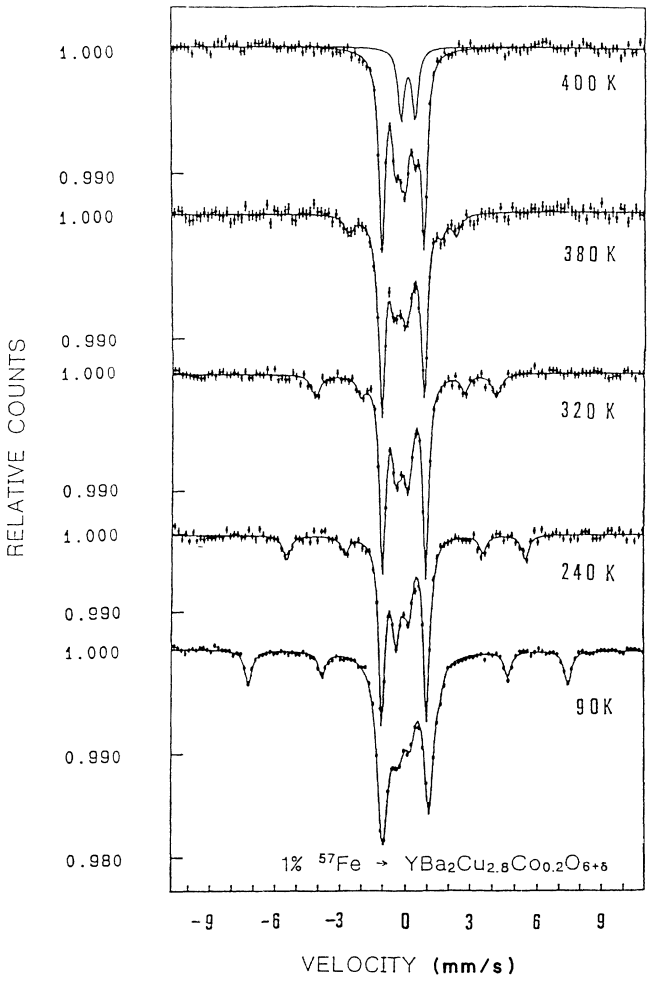

FIG. 3. Mössbauer spectra of $YBa_2Cu_{2.8}Co_{0.2}O_{6+\delta}$ at various temperatures. Note the additional doublet at 400 K (above T_N) corresponds to the Cu(2) site.

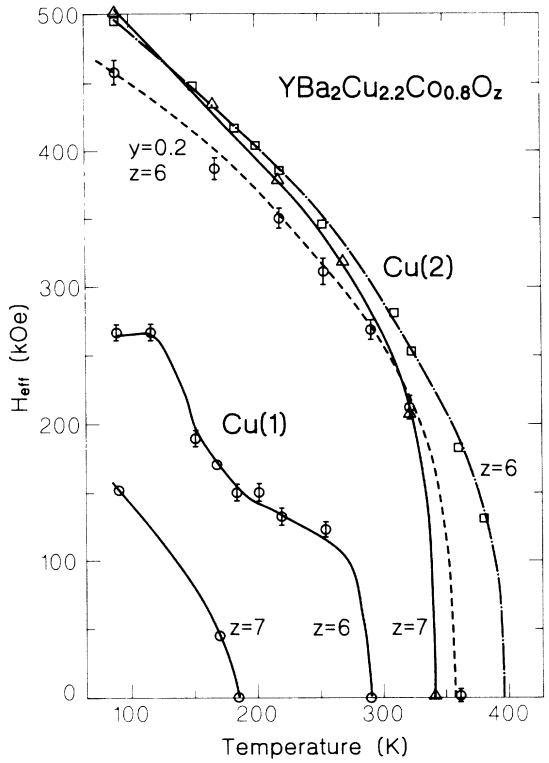

FIG. 4. Temperature dependence of the magnetic hyperfine field acting on ^{57}Fe in Cu(2) and Cu(1) sites in $YBa_2Cu_{2.2}Co_{0.8}O_z$. The dashed line corresponds to $YBa_{2.8}Cu_{2.8}Co_{0.2}O_{6+\delta}$.

site. On the other hand, the absence of superconductivity in both oxygen-rich and oxygen-deficient samples induces magnetic order in the Cu(2) sites. Neutron-scattering studies[12,15] of oxygen-deficient $YBa_2Cu_{2.2}Co_{0.8}O_{6+\delta}$, show indeed an ordered moment on both Cu sites, but only a single transition temperature at 435 K was observed.

The Mössbauer spectra at different temperatures obtained in $YBa_2Cu_{2.2}Co_{0.8}O_{6+\delta}$ are shown Fig. 5. At 90 K, the spectrum shows a complicated structure. We attribute this spectra to two magnetic sites with magnetic hyperfine fields of $H_{eff}(1)=493(5)$ kOe and $H_{eff}(2)=265(5)$ kOe with relative intensities of 28% and 59% respectively. The $H_{eff}(1)$ value, which is similar to that obtained for $y=0.2$ (Fig. 4), corresponds to Fe in the Cu(2) sites and $H_{eff}(2)$ to Fe in the Cu(1) site.

To get a better fit to the spectra at 90 K two additional doublets, which account for about 7% and 6% of the spectral area, were added with $S_{IS}=0.49$ and 0.2 mm/s and $\frac{1}{2}eqQ=0.69$ and $\frac{1}{2}eqQ=2.15$ mm/s respectively. The second doublet is similar to that obtained for the square planar configuration [Fig. 2(a)] and the first is very likely to be influenced by Fe (Co) clustering occurring at high concentrations.[14] The main effect to be seen in Fig. 5 is an increase of the central part of spectra when the temperature is increased. This is due to the change in the size of the hyperfine field of $H_{eff}(2)$. A Néel temperature of 300±20 K is obtained for the Cu(1) site. Above 300 K, the linewidth of the central part practically does not change and one still observes the magnetic lines which are related to Fe in the Cu(2) sites. We obtain $T_N=435$ as the Néel temperature of the Cu(2) sites (Table I). The general behavior of the magnetic nature of the Cu(2) site is consistent with our previous work on $YBa_2Cu_3O_6$.[4] Generally speaking the same behavior is observed also in the oxygen-rich $YBa_2Cu_{2.2}Co_{0.8}O_{7+\delta}$ sample (Fig. 6). Two independent magnetic transitions corresponding to Cu(1) and Cu(2) at $T_{N1}=380$ K and $T_{N2}=200(20)$ K with $H_{eff}(1)=500$ kOe and $H_{eff}(2)=152$ kOe at 90 K are observed (Table I). Figure 4 shows the hyperfine fields of the two sites as a function of temperature in the different samples. The temperature dependence of the Fe hyperfine field in the Cu(2) site is found to be identical for all systems if the normalized $H_{eff}(T)/H_{eff}(0K)$ is plotted versus the reduced temperature (T/T_N).[16] Note the unusual variation of H_{eff} for the Cu(1) site in $YBa_2Cu_{2.2}Co_{0.8}O_{6+\delta}$ (Fig. 4).

Remarkably our present results are completely different from those reported by Miceli *et al.*[15] In their work for $YBa_2Cu_{2.2}Co_{0.8}O_{6+\delta}$ a single transition is observed at $T_N=435$ K which corresponds to both Cu(1) and Cu(2) sites, whereas our results indicate clearly the

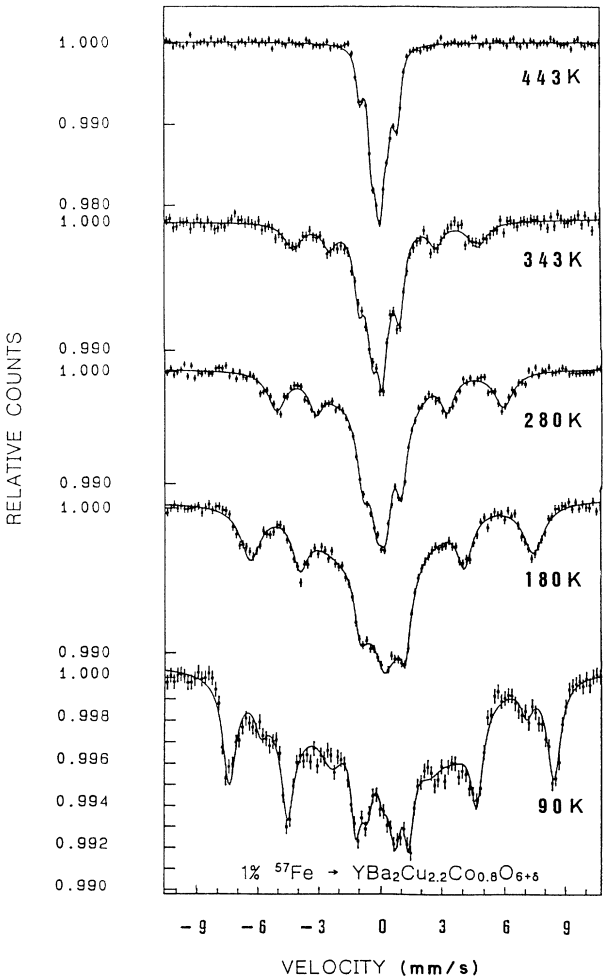

FIG. 5. Mössbauer spectra of ^{57}Fe in $YBa_2Cu_{2.2}Co_{0.8}O_{6+\delta}$ at several temperatures.

existence of two uncoupled sublattices with different transition temperatures. Two transitions are observed for the fully oxygenated sample also but with lower transition temperatures. This is a surprising result as (for $z=6$) the Cu on the chain site is expected to be monovalent[17] and for $z>6$ the amount of divalent Cu increases and a higher T_N for Cu(1) is expected. However, it seems that here, with such a large occupancy of the Cu(1) site by the magnetic Co ion, the magnetic properties of this site are dictated by the magnetic dopant and not by the magnetic properties of the Cu(1) ion. The situation is different in the Cu(2) site where the concentration of Fe or Co is only 20% of that in the Cu(1) site. The origin and nature of the chain-site magnetic ordering is still not clear.

D. Phase diagram of $YBa_2Cu_{3-y}Fe_yO_{7+\delta}$

Substitution of Fe for Cu has drawn much attention due to the possibility of evaluating the role of magnetic ions in the superconducting mechanism and because Mössbauer measurements on ^{57}Fe provide direct, useful information on the local environment of Fe. Substitution of Fe in $YBa_2Cu_3O_7$ results in an orthorhombic-tetragonal structure transition for $y=0.05$. Like Co, Fe replaces Cu preferentially in the Cu(1) sites,[10] and for higher concentration ($y>0.05$)10–20% of Fe also occupies the Cu(2) sites. The substitution of Cu by Fe produces drastic changes in T_c. Several groups measured the variation of T_c with y and the change of T_c with y obtained by different groups differs somewhat from group to group. These differences simply arise from the synthesis history of the samples. All the reported results lie within an upper and lower bound limit and it is well established that T_c remains constants and equal to 90 K up to the orthorhombic-tetragonal transition and then decreases continuously to less than 4.2 K at $y>0.4$. The mean values for the dependence of T_c on y is shown in Fig. 7. Upon increasing y further, the compounds become semiconductors and our Mössbauer measurements show that simultaneously antiferromagnetism associated with the Cu(2) ions develops. The solubility limit of Fe in $YBa_2Cu_3O_7$ is $y=0.8$.

Figure 8 exhibits the Mössbauer spectra of the oxygen-rich $YBa_2Cu_{2.25}Fe_{0.75}O_{7+\delta}$ and T_N is defined in the same manner as described previously for M=Co. In the samples with $y=0.5$ and $y=0.75$ at 90 K we observe a well-defined magnetic sextet which accounts for about 17% and 26% of the spectral area, respectively. Here again, this sextet is attributed to iron which replaces copper in the Cu(2) sites and orders antiferromagnetically. [Note the increase of the fraction of Fe in the Cu(2) site with increasing Fe content in the sample.] In that respect $YBa_2Cu_{2.25}Fe_{0.75}O_{7+\delta}$ differs from the oxygen-rich $YBa_2Cu_{2.2}Co_{0.8}O_{7+\delta}$ compound (Fig. 6) where the two Cu sites are magnetically ordered at 90 K. It should be noted that here again a magnetic sextet of the Cu(2) site is obtained in oxygen-rich samples and no magnetic structures are obtained in the superconducting range where $y<0.40$.

The central part of the Mössbauer spectra obtained for $YBa_2Cu_{2.25}Fe_{0.75}O_{7+\delta}$ at 90 K is shown on an extended

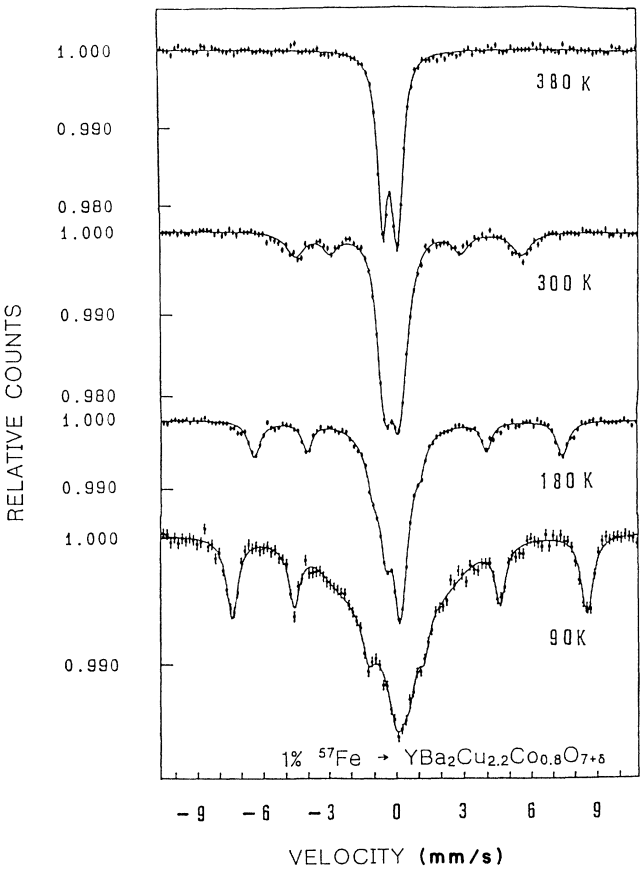

FIG. 6. Mössbauer spectra of ^{57}Fe in $YBa_2Cu_{2.2}Co_{0.8}O_{7+\delta}$ at several temperatures.

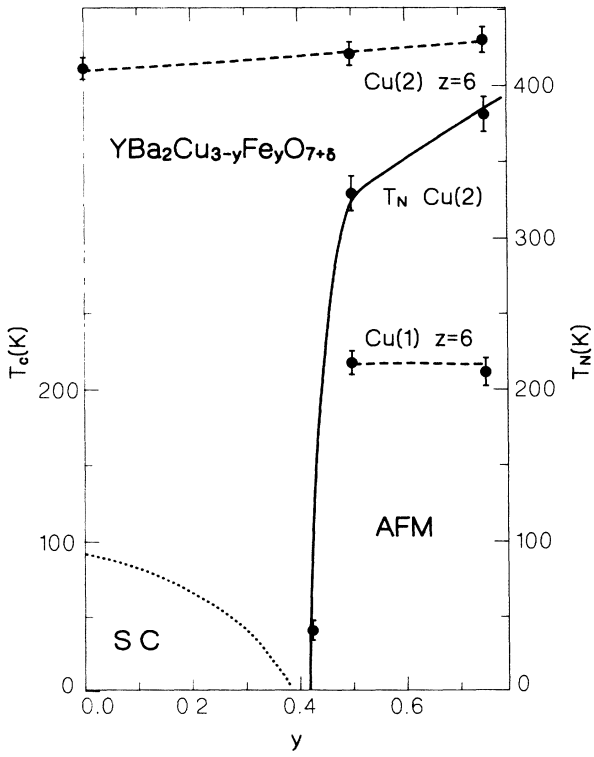

FIG. 7. Superconducting-magnetic phase diagram for the oxygen-rich $YBa_2Cu_{3-y}Fe_yO_{7+\delta}$. The dashed lines show T_N values for the quenched samples in both sites.

scale in Fig. 9. The large quadrupole splitting of $\frac{1}{2}eqQ = 1.99$ mm/s is associated with square planar coordinated Fe [Fig. 2(a)] and the pyramidal configuration with $\frac{1}{2}eqQ = 1.09$ mm/s [Fig. 2(b)] is the most intense subspectra (49%). The intensity of the octahedral structure [Fig. 2(d)] with $\frac{1}{2}eqQ = 0.37$ mm/s is 23%. The last subspectrum with $\frac{1}{2}eqQ = 0.50$ mm/s and $S_{IS} = 0.004$ mm/s is very likely to be expected for Fe clustering occurring at these high concentrations.[14] Figure 9 also shows the inner two lines of the magnetic sextet corresponding to the Cu(2) site. The relative intensities of the various subspectra are very similar to those obtained with 1% Fe doped in oxygen-rich $YBa_2Cu_3O_7$, and are almost independent of the iron concentration. They are determined only by the probability of each oxygen configuration.

In Fig. 7 the change of T_N as a function of y is displayed. T_N decreases gradually from 390 K for $y = 0.75$ to 330 K for $y = 0.50$ and then drops sharply to 29 K for $y = 0.45$. The T_N value for $y = 0.45$ was obtained by direct magnetization measurements to be discussed below. The SC-AFM phase diagram exhibited in Fig. 7 for $YBa_2Cu_{3-y}Fe_yO_{7+\delta}$ is very similar to that obtained for $Y_{1-x}Pr_xBa_2Cu_3O_7$ (Ref. 5) and YBa_2CuO_z.[3] All these examples indicate that AFM is commonly found at concentrations where superconductivity disappears, which means that the materials exhibit either superconductivity, or antiferromagnetic order, depending on composition. There is no evidence for coexistence of both phenomena at the same composition (Fig. 7).

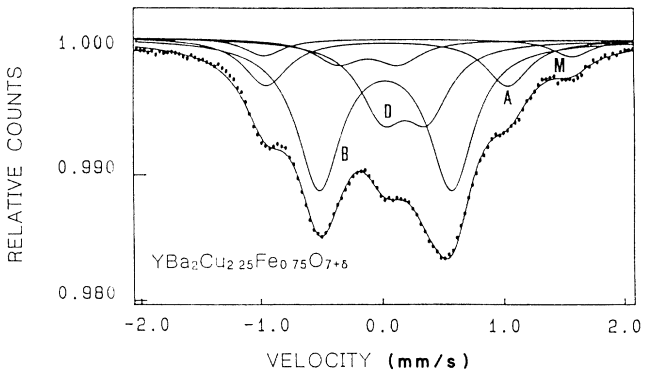

FIG. 9. The Mössbauer spectra of $YBa_2Cu_{2.25}Fe_{0.75}O_{7+\delta}$ at 90 K on an extended velocity scale. The symbols *A*, *B*, and *D* are related to planar, pyramidal, and octahedral configuration of Fig. 2 and *M* corresponds to the magnetic lines (see the text).

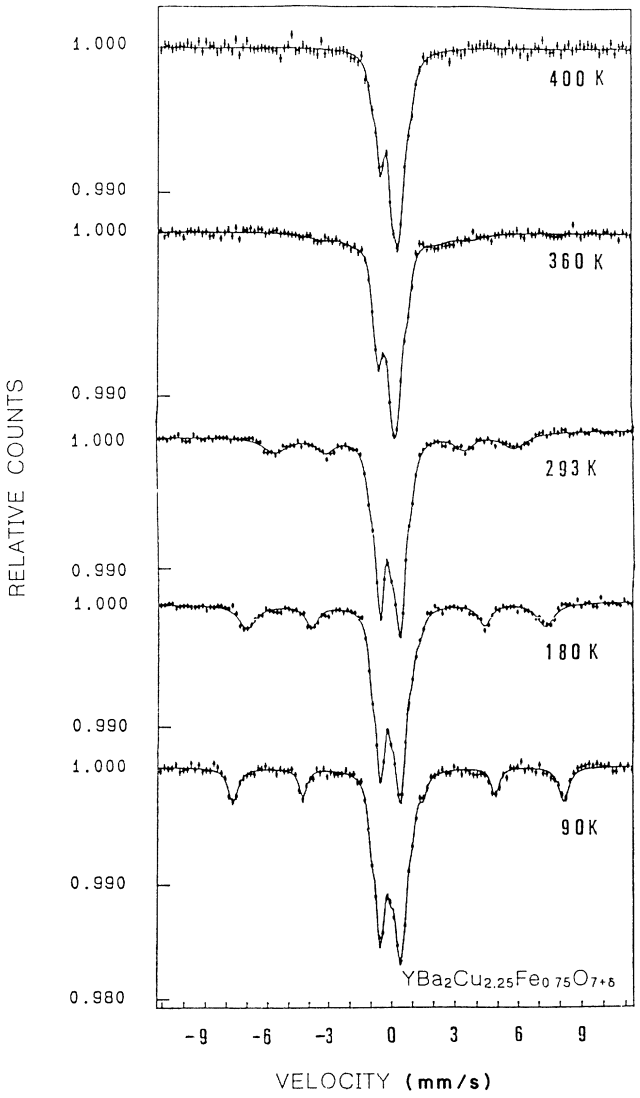

FIG. 8. Mössbauer spectra of $YBa_2Cu_{2.25}Fe_{0.75}O_{7+\delta}$ at several temperatures.

T_N for $y = 0.45$ was obtained by magnetization measurements. The temperature dependence of the field-cooled magnetization curve in 1 kOe (Fig. 10) shows a cusplike anomaly at 29 K which is superimposed on a paramagnetic component. The temperature dependence of the susceptibility between 30 and 190 K is well characterized by the Curie-Weiss law $\chi = \chi_0 + C/T - \Theta$, where χ_0 is the temperature-independent susceptibility and C and Θ are the Curie constant and Weiss temperature, respectively. The values obtained by least-squares fits are $\chi_0 = 1 \times 10^{-6}$ emu/g, $C = 4 \times 10^{-4}$ emu/g, and $\Theta = -2.1$

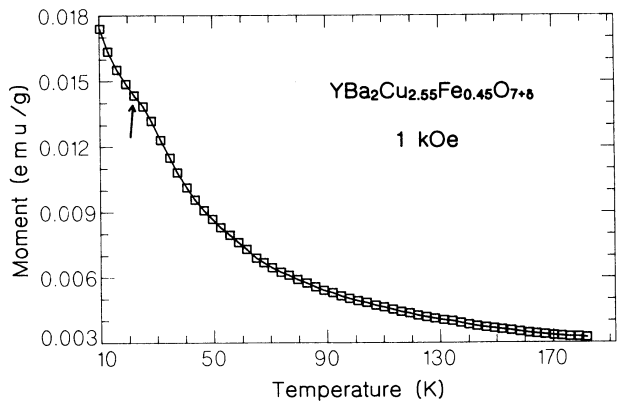

FIG. 10. Field-cooled magnetization curve at 1 kOe for $YBa_2Cu_{2.55}Fe_{0.45}O_{7+\delta}$.

K. Our data are in perfect agreement with those obtained in Ref. 18. The deviation from the Curie-Weiss law occurs at about 29 K, which is therefore assumed to be T_N of the sample. Since no magnetic ordering of Cu(1) sites is observed in oxygen-rich samples *even* for higher Fe concentrations (Fig. 8), it follows that $T_N = 29$ K is the Néel temperature of the Cu(2) sites for $y = 0.45$

E. Magnetic structure of the quenched $YBa_2Cu_{3-y}Fe_yO_{6+\delta}$

Two independent magnetic transitions are observed in the oxygen-deficient $YBa_2Cu_{3-y}Fe_yO_{6+\delta}$ compounds. Figure 11 exhibits the Mössbauer spectra for $YBa_2Cu_{2.25}Fe_{0.75}O_{6+\delta}$ obtained at different temperatures. As in the case of $YBa_2Cu_{2.2}Co_{0.8}O_z$ (Fig. 5), the spectrum at 90 K is a complicated spectrum with two magnetic sites. The magnetic hyperfine field $H_{\text{eff}}(1) = 495$ kOe with relative intensity of 37% and $S_{\text{IS}} = 0.40$ mm/s corresponds to Fe in the Cu(2) sites which order at 430 K, and the second hyperfine $H_{\text{eff}}(2) = 296$ kOe with relative intensity of 43% and $S_{\text{IS}} = 0.26$ mm/s corresponds to Fe in the Cu(1) site which orders at 210 K. Here again, two additional quadrupole splittings with $\frac{1}{2}eqQ = 2.30(2)$ and 1.32(2) mm/s and $S_{\text{IS}} = 0.03$ and 0.36 mm/s with relative intensities of 12% and 9%, respectively, were added to obtain a better fit to the spectra. The Néel temperature of the Cu(1) site was determined in the same way as for $YBa_2Cu_{2.2}Co_{0.8}O_{6+\delta}$ (see previous discussion). Mössbauer spectra for $y = 0.5$ (not shown) are very similar to Fig. 11. Figure 7 shows that the Néel temperature of both Cu(1) and Cu(2) sites change very little with y for $y \geq 0.5$.

Figure 12 summarizes the hyperfine fields of both sites as a function of temperature in the different samples. The collected evidences indicate that in the $YBa_2Cu_3O_7$ system the competition between superconductivity and magnetism leads to the appearance of one phenomena whenever the second disappears. Preliminary experiments on nominally oxygen-deficient compounds containing a low concentration of ($y \leq 0.1$) of Zn in $YBa_2Cu_{3-y}Zn_yO_z$ exhibit different magnetic behavior. Divalent Zn substitutes both Cu sites whereas trivalent Fe or Co substitute mainly the Cu(1) site.[10] The general result is that substituting small amounts of Zn for Cu strongly inhibits superconductivity and doping of 8% Zn drives T_c to zero. This implies that T_c is more affected when the doping occurs in the CuO_2 planes than in the CuO chains and therefore that superconductivity is confined to the CuO_2 planes. Zn is a unique dopant in that the fully oxygenated samples, which are not superconducting ($y = 0.1$), do not show magnetic ordering in the CuO_2 planes. Moreover, the magnetic ordering temperatures T_N of the oxygen-deficient samples depend on Zn concentration (unlike the systems shown in Figs. 5 and 7) and antiferromagnetism disappears approximately at the same concentration ($y = 0.25$) where superconduc-

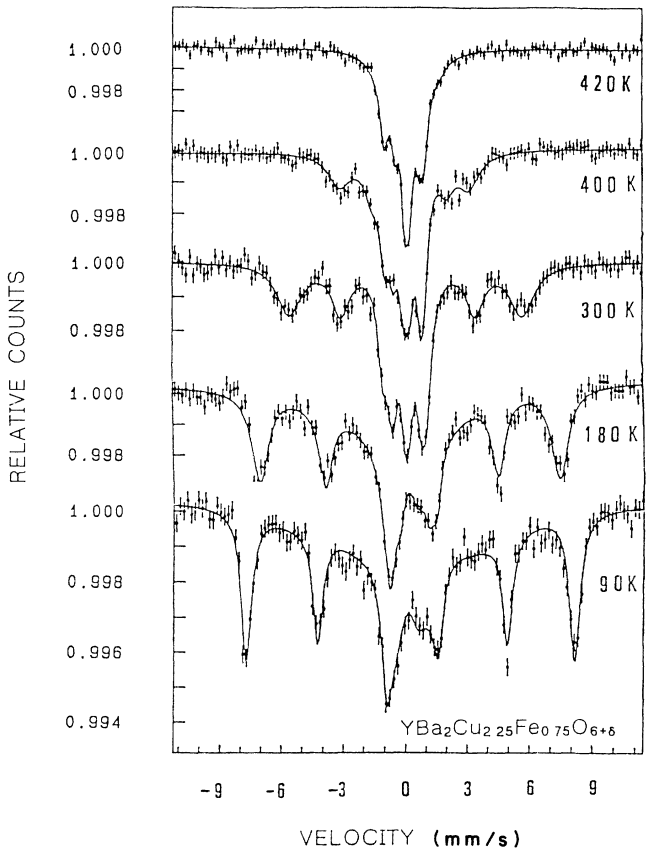

FIG. 11. Mössbauer spectra of $YBa_2Cu_{2.25}Fe_{0.75}O_{6+\delta}$ at various temperatures.

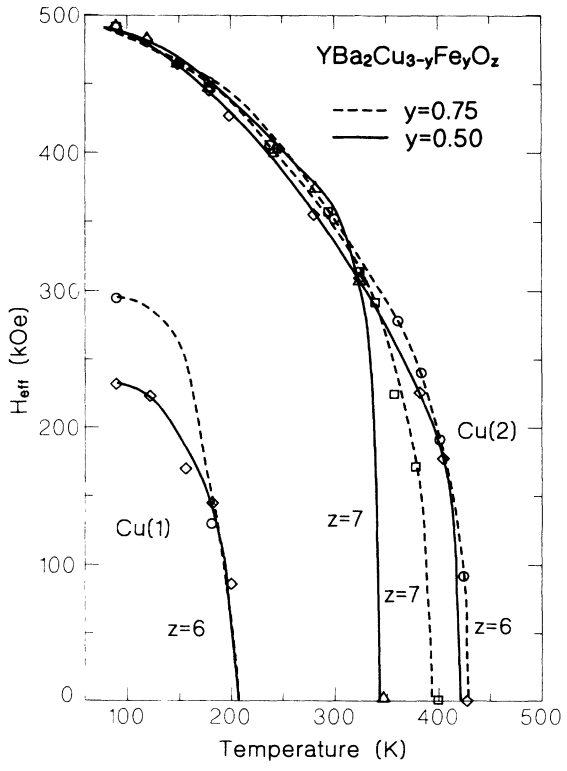

FIG. 12. Temperature dependence of the magnetic hyperfine field acting on ^{57}Fe in Cu(2) and Cu(1) sites in $YBa_2Cu_{3-y}Fe_yO_z$.

tivity for the oxygen-rich samples is destroyed. The absence of static magnetic order in the region of high Zn concentration in both fully oxygenated and quenched samples clearly demonstrates that Zn can inhibit superconductivity in the same way that it reduces long-range magnetic correlations. Understanding this behavior of substitution in the CuO_2 planes will give some additional insight into the fundamental interactions in the CuO_2 planes. This research is now in progress.

IV. CONCLUSION

Based on the studies reported here we can summarize the behavior of the $YBa_2Cu_{3-y}M_yO_z$ systems as follows: (a) For $z=7$ the system is superconducting for $y<0.4$ values, but antiferromagnetic at the Cu(2) site for high values of y. (b) There is no unambiguous observable evidence for overlap of superconductivity and antiferromagnetism. (c) For $z=6$ the Cu(2) site is antiferromagnetic for all y values and T_N varies little with y: $T_{N1}\sim 420$ K. (d) For $z=6$ and $y\geq 0.5$ the Cu(1) site is also magnetically ordered with $T_{N2}=220$ K and the two magnetic sublattices are decoupled. (e) In the oxygen-rich $YBa_2Cu_{2.2}Co_{0.8}O_{7+\delta}$ two magnetic sublattices are found, but with lower Néel temperatures.

It turns out that in the substituted $YBa_2Cu_3O_7$ system whenever superconductivity disappears the Cu(2) sites become magnetically ordered. The mechanism for the magnetic behavior of this system is still not clear.

ACKNOWLEDGMENTS

We are grateful to R. Hareuveny at the Physics Department, Bar-Ilan University for the magnetization measurements of $YBa_2Cu_{2.55}Fe_{0.45}O_{7+\delta}$. This research was supported by a grant from the German-Israel Foundation (GIF) for Scientific Research and Development Grant No. I-40-100.10/87 and by a grant from the United States-Israel Binational Science Foundation (BSF), Jerusalem, Israel.

[1]P. W. Anderson, Science **235**, 1196 (1987); V. J. Emery, Phys. Rev. Lett. **58**, 2794 (1987).

[2]J. M. Tranquada, D. F. Cox, W. Kunnmann, H. Moudden, G. Shirane, M. Suenaga, P. Zolliker, D. Vaknin, S. K. Sinha, M. A. Alvarez, A. J. Jacobson, and D. C. Johnston, Phys. Rev. Lett. **60**, 156 (1988).

[3]D. C. Johnston, S. K. Sinha, A. J. Jacobson, and J. M. Newsam, Physica C **153-155**, 572 (1988).

[4]I. Nowik, M. Kowitt, I. Felner, and E. R. Bauminger, Phys. Rev. B **38**, 6677 (1988).

[5]I. Felner, U. Yaron, I. Nowik, E. R. Bauminger, Y. Wolfus, E. R. Yacoby, G. Hilscher, and N. Pillmayer, Phys. Rev. **40**, 6739 (1988).

[6]D. Vaknin *et al.*, Phys. Rev. Lett. **59**, 1045 (1987).

[7]T. Oashi, K. Kumagai, Y. Nakajima, T. Tomita, and T. Fujita, Physica C **157**, 315 (1989).

[8]R. F. Kiefl *et al.*, Phys. Rev. Lett. **63**, 2136 (1989).

[9]P. H. Hor, R. L. Meng, Y. Q. Wang, L. Gao, Z. J. Huang, J. Bechtold, K. Forster, and C. W. Chu, Phys. Rev. Lett. **58**, 1891 (1987).

[10]R. W. Howland, T. H. Geball, S. S. Laderman, A. Fischer-Colbrie, M. Scott, J. M. Tarascon, and P. Barboux, Phys. Rev. B **39**, 9017 (1989).

[11]I. Felner, I. Nowik, and Y. Yeshurun, Phys. Rev. B **36**, 3823 (1987).

[12]P. F. Miceli, J. M. Tarascon, P. Barboux, L. H. Greene, B. G. Bagley, G. W. Hull, M. Giroud, J. J. Rhyne, and D. A. Neumann, Phys. Rev. B **39**, 12 375 (1989).

[13]E. R. Bauminger, M. Kowitt, I. Felner, and I. Nowik, Solid State Commun. **65**, 123 (1988).

[14]E. B. Saitovitch, R. B. Scorzelli, I. S. Azevedo, and H. Micklitz, Phys. Rev. B **41**, 2103 (1990).

[15]P. F. Miceli, J. M. Tarascon, P. Barboux, L. H. Greene, M. Giroud, D. A. Neumann, and J. J. Rhyne, Phys. Rev. **38**, 9209 (1988).

[16]I. Nowik, G. Kaindl, E. R. Bauminger, I. Felner, M. Kowitt, and U. Yaron (unpublished).

[17]J. M. Tranquada, S. M. Heald, A. R. Moodenbough, and Y. Wu, Phys. Rev. B **38**, 8720 (1988).

[18]S. Katano, T. Matsumoto, A. Matsushita, T. Hatamo, and F. Funahashi, Phys. Rev. B **41**, 2009 (1990).